

# Impact of Artificial Light at Night on Bird Migration

Emily Hansen<sup>1</sup>, Cheng Ma<sup>2</sup>, Matthew Dwyer<sup>3</sup>, Greg Dobler<sup>2</sup>, and Christian Moscardi<sup>1</sup>

<sup>1</sup>New York University Shanghai

<sup>2</sup>Affiliation not available

<sup>3</sup>NYU Center for Urban Science & Progress

May 10, 2021



Figure 1: It

## 2018 Capstones

### Abstract

Millions of birds are killed annually as a result of collisions with buildings or exhaustion from being disoriented and trapped by intense artificial light (Crawford and Engstrom 2001). The problem is especially pronounced in urban areas, during migration season, and during times when anomalously large amounts of man-made light are emitted at night. Previous research has shown that there is an association between light and bird flight paths at low spatio-temporal resolution (La Sorte et al., 2017) as well as at a very granular spatial resolution during specific temporal events (Van Doren et al., 2017). However, there is a notable lack of research addressing neighborhood-scale flight and death patterns in urban areas. Here we develop statistical and spatial analyses of the relationship between reflectivity as a proxy for migratory birds and photogrammetrically mapped light intensity levels at a high spatio-temporal resolution in Manhattan. From there, we aim to correlate

bird death counts at specific buildings to these increased light levels. The findings of this project demonstrate no conclusive positive or negative correlation between reflectivity and building brightness, but do suggest variation at a local scale and clear temporal patterns in aggregate.

## 1 Introduction

The airspace above major urban centers all over the world are home to millions to billions of migratory land bird migrations annually. The majority of this migration activity occurs overnight, where birds have evolved to rely on electromagnetic signals and light sources, such as stars, for navigation. Over urban areas, however, artificial light at night (ALAN) attracts the attention of migratory birds and disrupts their flight patterns. As light pollution increases, mass bird mortality at lighted structures has become increasingly documented, with ALAN associated with flight path deviation (La Sorte et al., 2017).

The project will combine three disparate data sets and perform the following: photogrammetric analysis of ALAN emissions from buildings in Manhattan using image data; identification and calculation of bird density in the air above the city from radar-derived observations; a statistical analysis of NYC Audubon-owned bird death count and location data in lower Manhattan; and a publicly-accessible visualization of each of the previous points. The ultimate goal of the project is to produce light maps of the area of interest, successful radar estimates of airborne bird density, an interactive visualization combining these data in a way that clarifies bird risk, and a series of experiments measuring the correlation of ALAN

and bird density, considering nights of both high and low overall brightness.

Previous work to quantify bird attraction to urban ALAN has been limited in spatial and temporal scales. One study investigated the effects of the 9/11 Memorial Tribute Lights in New York City on the behaviors of nocturnally migrating birds, finding that the annual event over seven years influenced the migration of 1.1 million birds (Van Doren et al., 2017). On the other hand, La Sorte et al. studied migration patterns across the northeast using satellite imagery to infer light levels and citizen science data to infer bird counts - while large in spatial scope, their study was limited in resolution. For example, light level “pixels” from the satellite data covered 3.3km<sup>2</sup> each (La Sorte et al., 2017).

More quantitative approaches to evaluate artificial light emissions at night have been performed in an urban context by Dobler et al., who utilized ALAN emissions from buildings in the New York City skyline to measure human behavior based on the identification of on/off light transitions. Patterns of light intensity and sudden shifts in average brightness of a building could be discerned with these methods (Dobler et al., 2015). The goal of this work is to determine if a similar pulse is present in bird counts over time and if that is geospatially and temporally correlated to the lighting variability.

## 2 Data and Methodology

### 2.1 Light Imaging and Photogrammetry

#### *Background*

The image data utilized for the duration of the study utilizes a collection of photographs taken by two cameras in the Bank of America Tower, located in Midtown Manhattan. This pair of cameras is responsible for recording the New York cityscape south into Lower Manhattan. Each night from 9PM-6AM, photos are taken every 10 seconds, with the complete collection over the past year nearing one million images and terabytes in size altogether. The cameras each have a 35-degree horizontal field of view, and produce images that are 3840 pixels wide and 5120 pixels high.

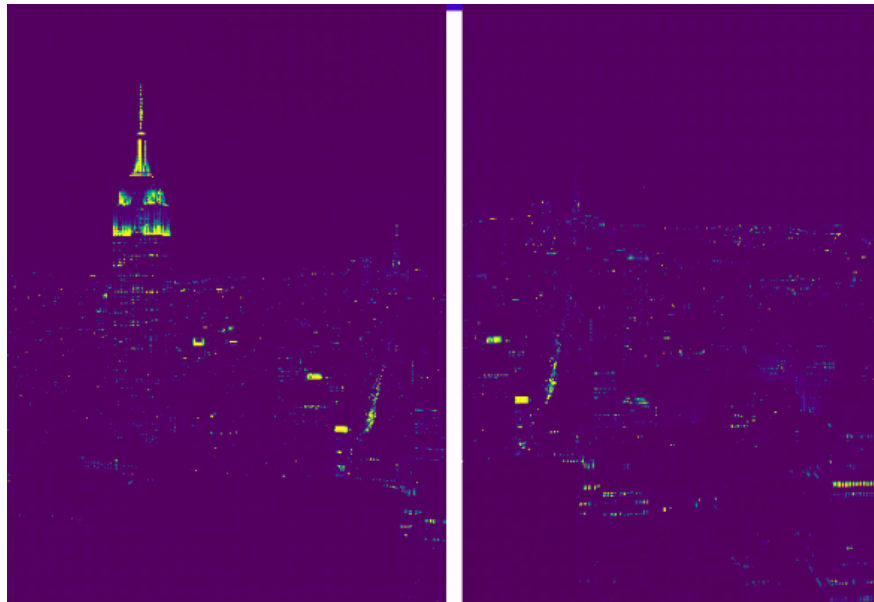


Figure 2: A pair of sample, raw images, taken 3 seconds apart, from the left-facing and right-facing cameras (respectively) in Midtown Manhattan. Colors are arbitrary to denote areas of brightness and darkness. Note the overlap between the two images in the “center”.

## *Methods*

The scene extent of the image data provides a generally comprehensive view of lower- to mid- Manhattan, and it is possible to extract the average light intensity of a building at night from these data. However, extracted information from the scene, such as ALAN intensity, is only useful for interpretability purposes if it can be mapped to building location or unique identifiers. For this reason, the imaging and photogrammetry portion of the project can be divided into three main parts: 1) projecting portions of the image onto individual building identifiers, 2) calculating average recorded brightness over those respective portions of the image corresponding to buildings, and 3) scaling the average brightness over each of these portions of the image, based on the projected building's surface area, to derive an estimate of the amount of light that particular building is emitting into the sky.

For 1), we followed the method outlined in (Schenck, 2005), using NYC 3D building model data as our source of information about the built environment, and including an approximation step to determine exactly how the camera was oriented in the 3D environment. Upon completing projection and calculating average brightness recorded at each building, we estimate overall light levels emitted from the building by the following formula:

$$B = B_{recorded} \cdot n\_floors \cdot perimeter$$

Where  $B$  is overall brightness,  $B_{recorded}$  is the average brightness over all pixels recorded by the camera for that building,  $n\_floors$  is the number of floors that building has (as reported by the NYC MapPLUTO dataset), and  $perimeter$  is the perimeter of the building's footprint (again derived from the NYC MapPLUTO dataset).

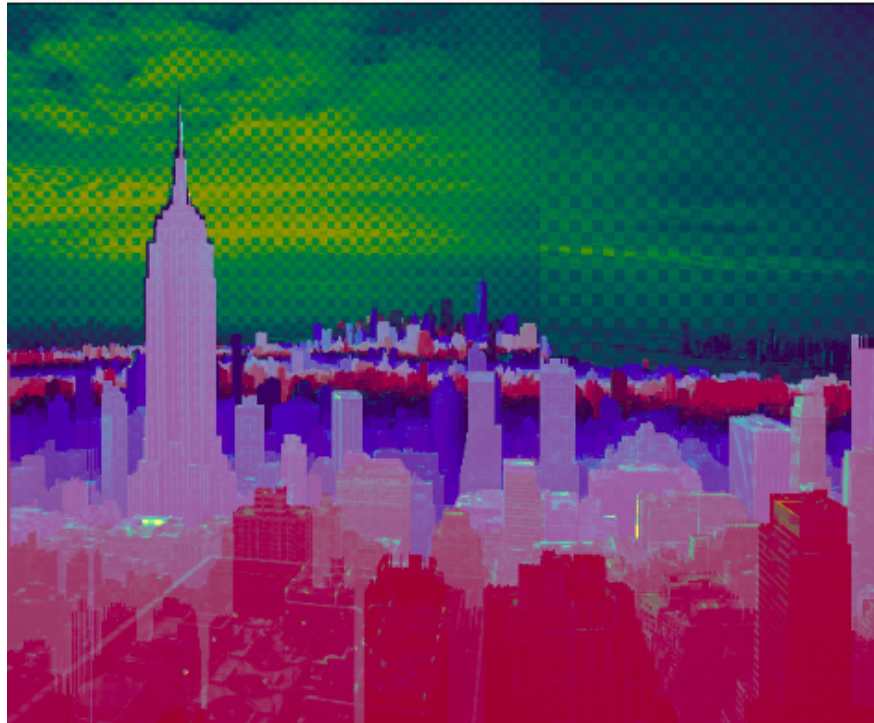


Figure 3: Result of step 1) - projection of 3D building data onto 2D images from the two cameras observing our area of interest. The level of visual agreement is decidedly very high. The cameras' fields-of-view have some overlap - this figure is the result of "stitching" those two photos into a contiguous field-of-view.

## 2.2 Radar Data and Bird Density Estimation

### *Background*

The radar data that will be utilized for the study is from the Weather Surveillance Radars-1988 Doppler (WSR-88D) network, also known as the Next Generation Weather Radar (NEXRAD)

system. NEXRAD comprises 160 radars around the United States, although the only installation that will be used in the study is KOKX, a radar located in central Long Island. The study will use publicly available Level-II data, with radar sweeps that are each approximately 10 minutes apart. The time range of processed radar data used for this project will be for 2017 to align with the collection of NYC building light imagery and Audubon volunteer data, and specifically night time (generally 9PM to 6 AM) for five days in September and October each, and 10 days in April. These month ranges were chosen because bird migration patterns are generally understood to occur in Spring and Autumn, with bird species, weather patterns, abundance of food, and flight routes all being factors that can influence the variation of timing in migration (Newton, 2008). The days selected were also made sure to have zero inches of precipitation, both to increase certainty of bird signals in the atmosphere as well as rain's reduction of clarity in the imaging of the Manhattan skyline. The precipitation data is sourced from a land based weather station in Central Park, NYC (NOAA, 2017).

### *Methods*

The radar scan used for this study is KOKX's lowest elevation angle of  $0.5^\circ$ , chosen because it will cover the most birds in the atmosphere. Due to the curvature of the Earth and the radar station's location, about 60 miles east of Manhattan, the  $0.5^\circ$  elevation scan passes above Manhattan at an altitude range of 0.7 to 2.4 km, with this range due to the  $\sim 1^\circ$  width of the radar beam itself (Van Doren, 2017; NOAA Radar Operations Center, 2017). Fall bird migration around New York has been found to occur in altitudes between

about 0.25 and 1.7 km, so the  $0.5^\circ$  scan angle, while overshooting, is the most encompassing of this migration range (La Sorte, 2015). Using an R based package called bioRad, NEXRAD grid cells of 100 meter squared areas over the study area in Manhattan are extracted from raw radar data, with each point containing information about relevant radar variables (Dokter, 2011). Three variables will be key to filtering the radar data to what can be more reliably assumed to be bird densities. The main variable of interest is reflectivity, measured in decibels relative to the reflectivity factor Z. The upper limit of reflectivity of birds is around 30 DBZ, so 35 DBZ will be chosen as a filter for the grid cells as a safe threshold (Stephanian, 2016). Other variables of interested are the copolar correlation coefficient (RHOHV), measuring the homogeneity of a sampled volume to filter meteorological observations from biological ones, and radial velocity, which can filter be used to filter immobile ground clutter. The specific ranges and descriptions of this methodology can be found in the supplemental section, and examples of these variables can be found in Figure 3.

To estimate bird density, a similar methodology to Gauthreaux et. al. will be employed. Gauthreaux was able to relate manual counts of birds crossing a 1.6 km line in an hour with dBZ from a radar's  $0.5^\circ$  elevation scan angles (the same angle utilized for this study) to create a linear fit line with an R-squared value of 0.87 (Gauthreaux et. al., 2008). The formula was then adjusted for this project (seen above) to accommodate different units, namely the study area conversions and of dBZ to Z, along with operating under assumptions of relating different migratory areas and times of year. The equation applied to each radar observation will be

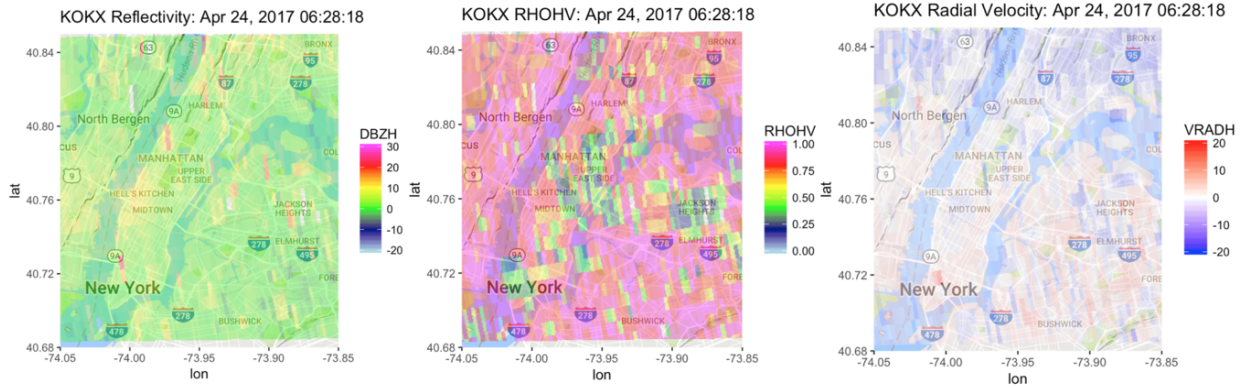


Figure 4: The results of a sweep from April 24th, 2017 at 6:28 AM. Reflectivity highlights densities in the atmosphere, RHOHV (a copolar correlation coefficient) shows where densities are irregular, and Radial Velocity shows the speed of objects relative to the radar. Based on overlap between the three, it is likely that birds appear in southern Manhattan, Central Park, and Jackson Heights.

able to estimate a number of birds within that area, which when summed will creating an estimation of total birds in the study area.

$$\frac{\text{Birds}}{100m^3} = \frac{\left(1.84 \cdot 10^{\frac{dBZ}{10}}\right)}{10}$$

### 2.3 Audubon Volunteer Data

#### *Background*

NYC Audubon provided data on bird deaths collected by volunteers over the span of about 7 months (April 1 2017 - November 11 2017). In total there were 26 volunteers who walked. To collect this data, each volunteer walked one of three routes in the early morning, several days of the week (there does not appear to be a clear pattern for which days the volunteers went out - likely each had a unique schedule). One of these routes was through midtown Manhattan, one through the west side of downtown Manhattan, and one through the east side of downtown Manhattan. Volunteers carefully examined perimeters of several high-risk (as identified by

NYC Audubon scientists) buildings along the route, looking for dead birds on the sidewalk, in shrubbery, or on low-hanging ledges. If a volunteer found a dead bird, they followed a specific protocol to identify, log, handle, and dispose of the dead bird. To ensure volunteer compliance and efficacy, NYC Audubon ran “gold standard” trials where they placed frozen dead birds on the sidewalk for volunteers to find. Volunteer accuracy was very high, though these trials were complicated by building maintenance and other cleanup workers collecting the dead birds before volunteers could find them.

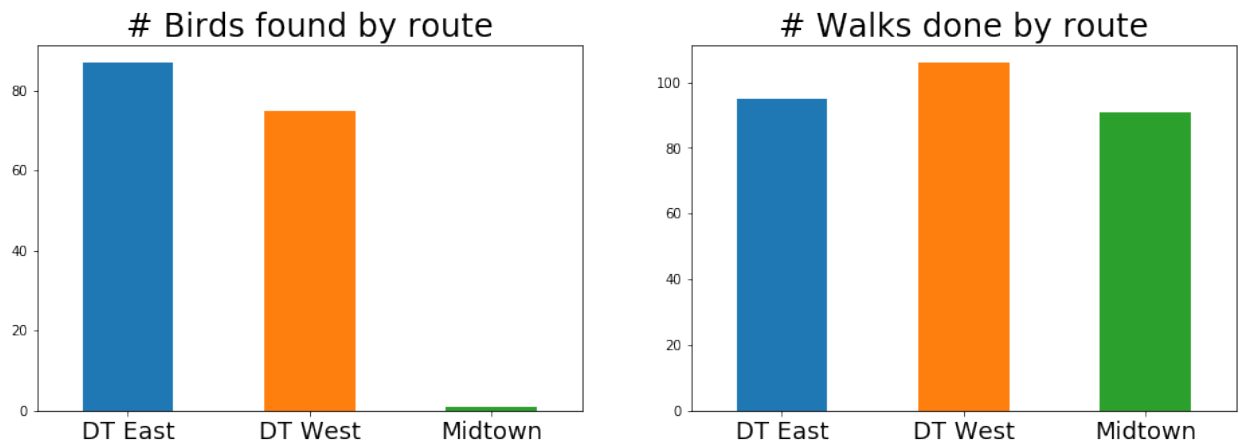


Figure 5: Left: Number of times each route was walked (out of 224 days). Right: total number of dead birds found along each route. Note that midtown had only 1 dead bird found during the entirety of the study.

## Methods

This data presented analytical challenges for two main reasons: first, the number of samples is quite small, and second, different volunteers may be better or worse at finding dead birds on different days. WRT the latter, aside from the gold standard trials, we were

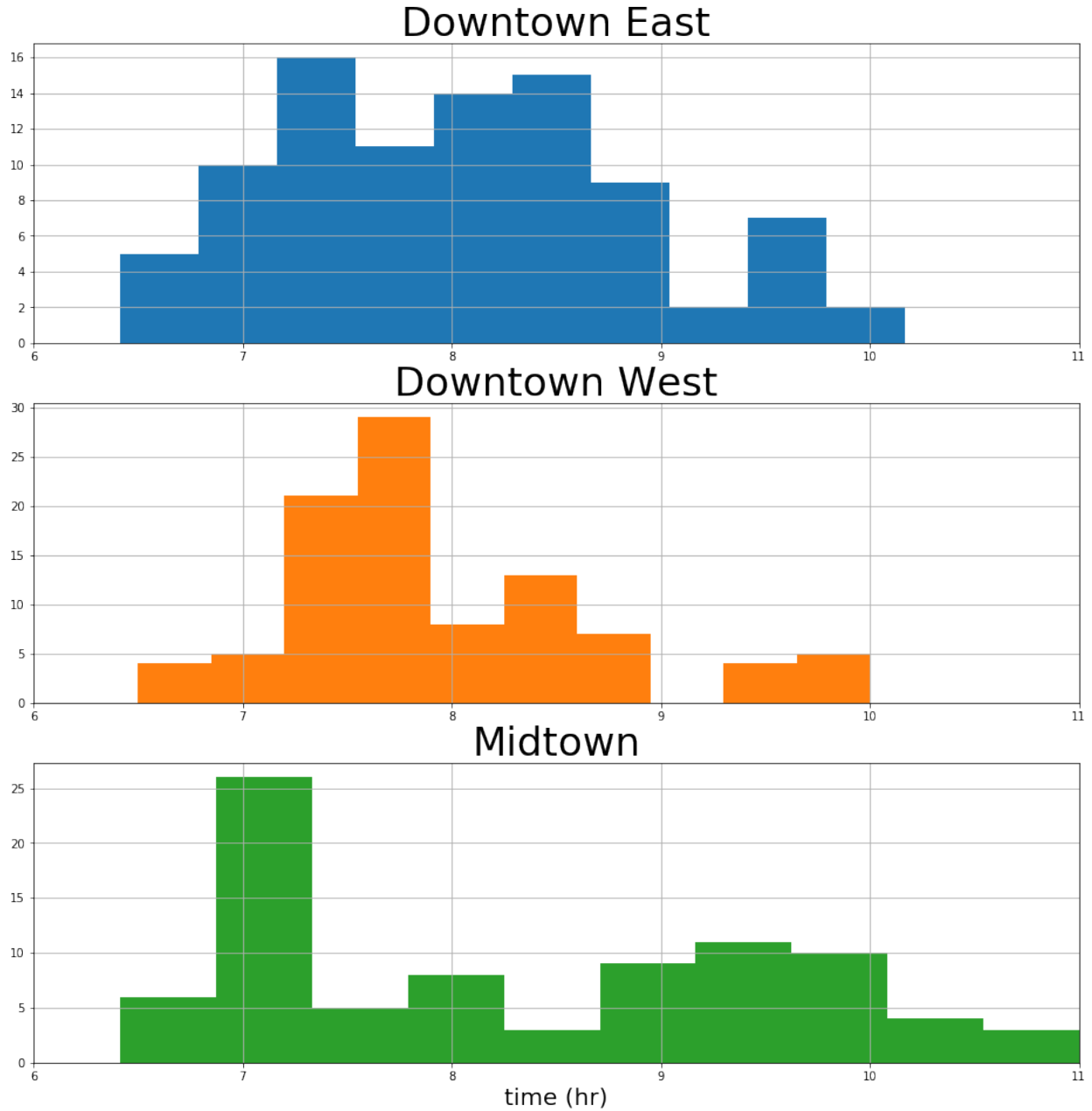


Figure 6: Histograms of times each route was walked. Note that the distribution of midtown times (bottom) is bimodal - with a mode at 7AM and another later in the morning (9-10AM). This may have impacted the midtown volunteers' ability to find dead birds.

able to verify that number of walks correlated directly with number of birds found - a good indication that volunteers perform relatively consistently on this task.

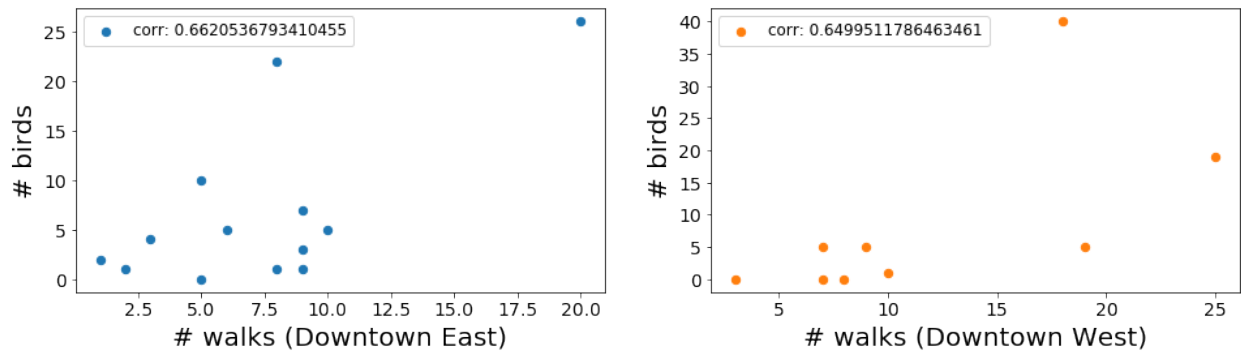


Figure 7: Total number of dead birds found vs. total number of walks taken by the NYC Audubon volunteers. Left: the Downtown East route. Right: The Downtown West route. In both cases we see that more walks corresponds to more dead birds found. This indicates volunteers perform consistently.

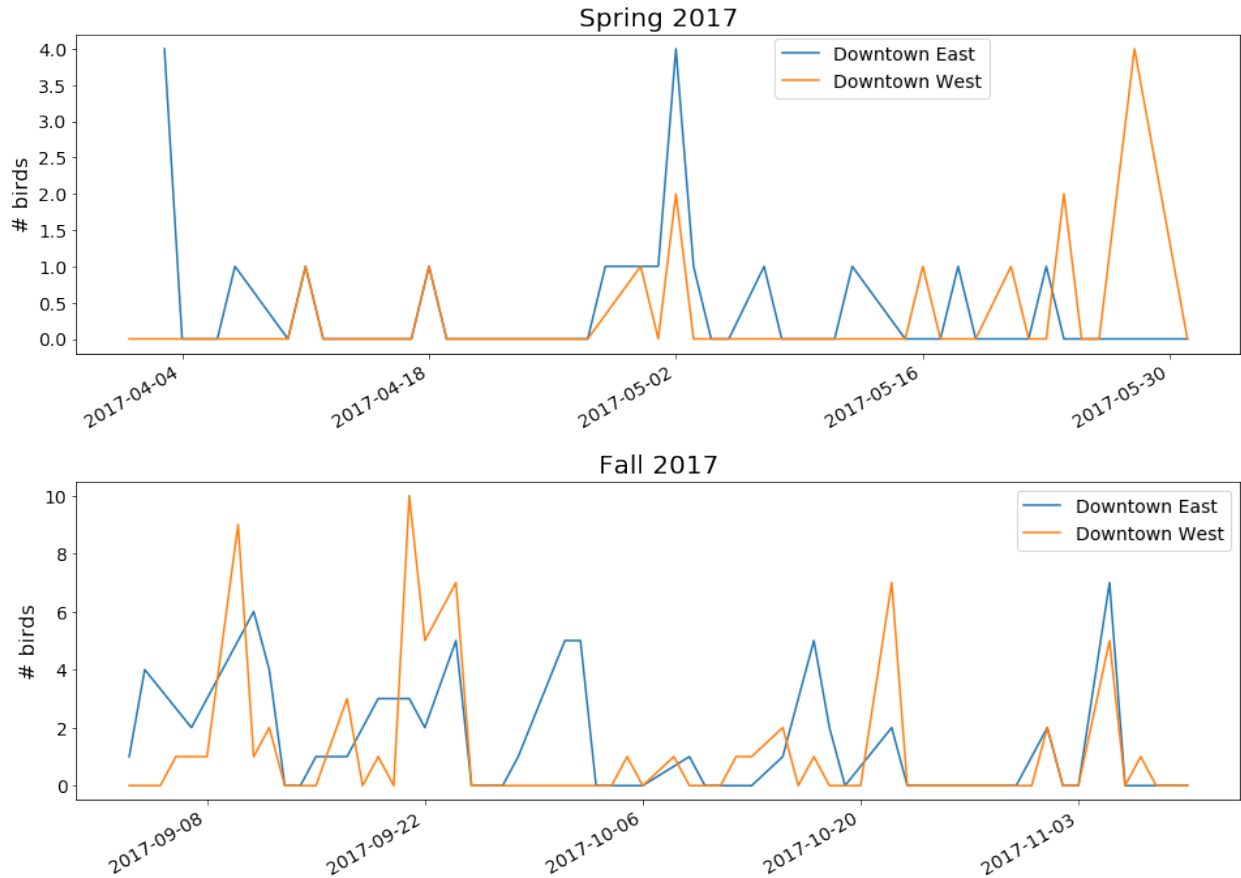


Figure 8: Number of dead birds found over time on each route (midtown excluded). Top: Spring 2017. Bottom: Fall 2017. Note that Fall 2017 had substantially more dead birds found in downtown Manhattan than did Spring 2017.

## 2.4 Joining Data

The building light and radar data are joined by selecting building centroids within a 200 foot radius of each radar observation and associating average lumination in that area with a measure of bird density in the atmosphere. This is done for each temporal record we have - the radar scans once every 10 minutes, each night. We encountered two main issues. First, some buildings are not visible to our cameras, such as buildings “behind” the Empire State Building. If such an occluded building fell within 200 feet of a radar observation, we picked the nearest building with a similar number of floors, and used its light measurement instead. If a set of spatial radar observations had no visible buildings within 200 feet, we did not use that observation in our analysis. Second, areas of radar scans with reflectivity below a certain amount lacked records in the dataset. To address this, we imputed bird density values of “0” for each such missing record. This allowed us to maintain spatial and temporal consistency as we tracked building lights over time, over our study area.

## 3 Results

### 3.1 Analysis in Aggregate

To explore the relationship between reflectivity and luminance, data were averaged in both study periods to the geography of the 100m<sup>2</sup> radar pixel, with the results plotted in Figure 8. The first statistical test run on the joined data was an ordinary least squares (OLS) regression, relating the independent variable of the log of lu-

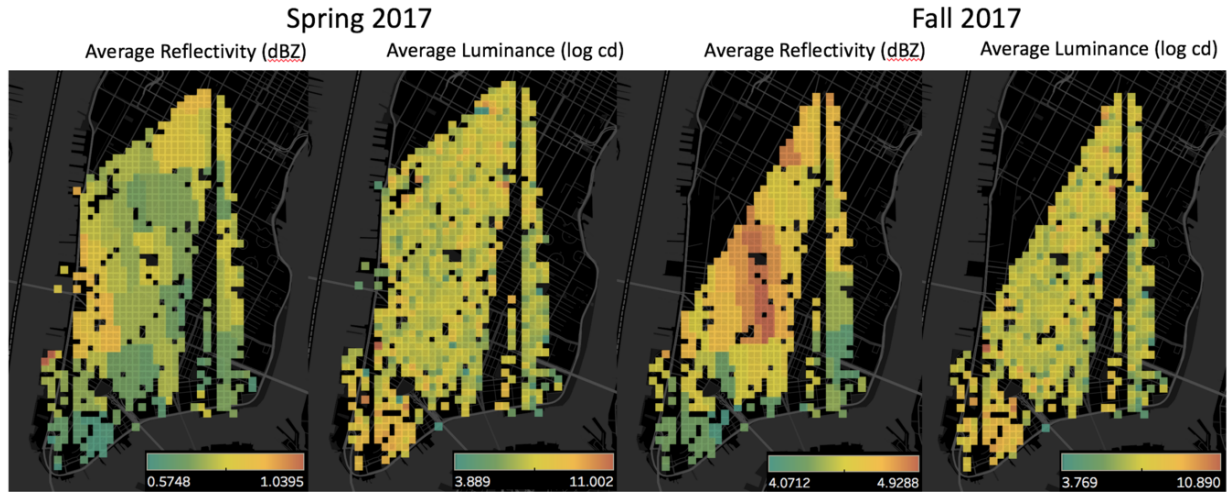


Figure 9: Reflectivity and building luminance averaged over 10 day periods in Spring and Fall 2017 for each radar pixel and nearby light. In aggregate, distributions of reflectivity vary, while luminance remains constantly higher in the Financial District and Midtown.

minance to the dependent variable reflectivity. The OLS regression for fall and spring yielded adjusted  $R^2$  values of 0.0008 and 0.004 respectively, meaning that either season’s model explains little of the variation of the data. The correlation coefficients for fall and spring are -0.011 and -0.02, along with a p-values of 0.21 and 0.02, indicating that for either model there is neither a particularly positive nor negative relationship between to the two variables. This finding was also found to be statistically insignificant in the fall, assuming a significance of  $p < 0.05$ .

However, because the use of linear regression relies on the assumption that the variables exhibit no spatial autocorrelation, a Global Moran’s I was run on both reflectivity and building lumination to determine the extent of autocorrelation (Poole, 1971). For reflectivity, a Moran’s I of 0.74 and 0.72 was found for Fall and Spring, along with a Moran’s I of 0.21 and 0.19 for logged lumination.

With p-values all below 0.01 for these spatial autocorrelation tests, both lumination and especially reflectivity were found to exhibit spatial autocorrelation. These findings mean local variation will need to be accounted for in a regression, so a spatial lag model was introduced, creating local regressions of reflectivity against lumination for each point based on a weights matrix of 3rd order and lower queen contiguity. The spatial lag model returned R-squared values of 0.8 and 0.79 for Fall and Spring, correlation coefficients of 0.001 and -0.008, and p-values of 0.6 and 0.03. Based on these results, the spatial lag model shows that there is high local variation between reflectivity and lumination, but in aggregate there is neither a positive or negative relationship between the two, so a closer investigation into the temporal components of the data will be needed to better understand the relationship.

### 3.2

### 3.3 Time Series Analysis

To first get a sense of these variables over time, dBZ is plotted over time along with building lumination estimates. Figure 9 shows a trend of average brightness decreasing overnight, while reflectivity increases later in the night and into the morning, suggesting night time migratory trends. When compared with Audubon collected data in Figure 7, there do not appear to be similar patterns in reflectivity and dead birds found, although given the limited spatial scope of the bird walks, this relationship remains inconclusive.

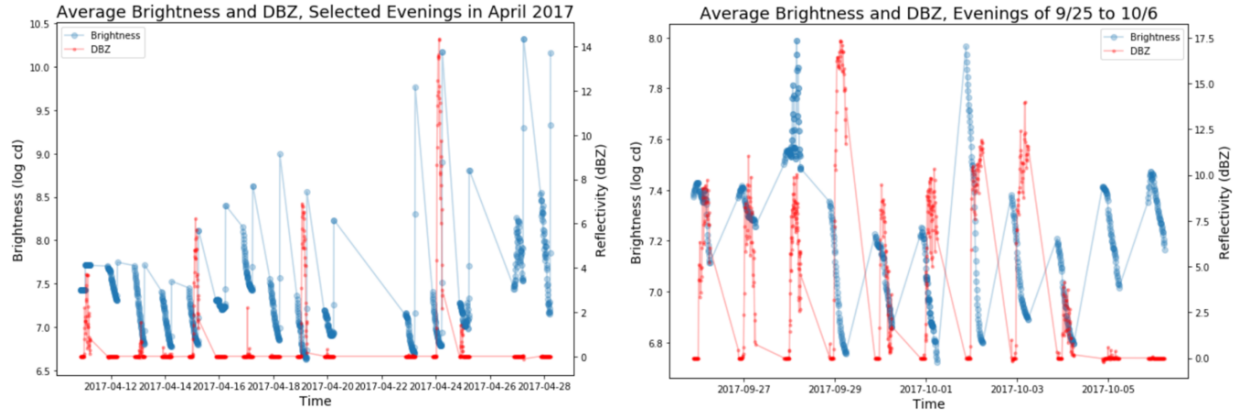


Figure 10: Brightness and reflectivity averaged over each timestamp in both seasons.

In addition to dBZ, bird counts were estimated from radar, for which a time series can be found in Figure 15 of the supplemental section. While difficult to verify, a baseline of about 100 birds was found in the study area, with night time peaks regularly reaching 700 - 2500 birds. As birds cannot be tracked and there not summed over time, this does give a preliminary view into the number of birds affected. Peaks are especially high in this time series due to the log nature of dbZ, with spikes in night time migration that are not unreasonably high given large bird estimates in other studies (Van Doren, 2017).

Next, bird density vs. brightness across space were correlated, at each time step. This helps answer the question of whether at any given instant in time, brighter areas are more (or less) likely to have more birds.

To further explore these variables, changes in bird density vs.

Correlations of B(t) and D(t), Fall 2017

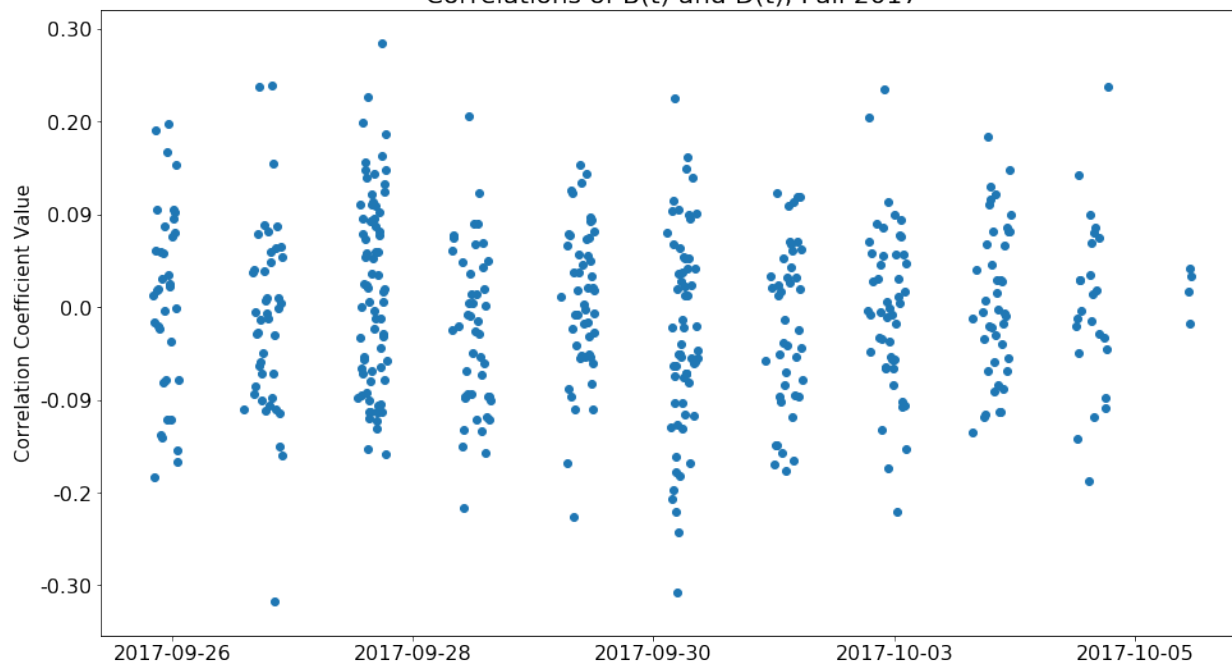


Figure 11: Correlations of bird density ( $D(t)$ ) and brightness ( $B(t)$ ) across space at each timestep where there was at least one nonzero bird density level, for 1.5 weeks in Fall 2017. The coefficients are uniformly distributed about 0 with no temporal pattern, indicating that given an area's relative brightness, it is hard to infer the expected bird density in that area.

changes in brightness in space, across time, were correlated. In particular, for time-steps when there was a nonzero change in brightness and bird density, did areas with increased or decreased brightness correlate to areas with increased or decreased bird density in that same time step. The resultant plot of spatial correlations between each time step is below.

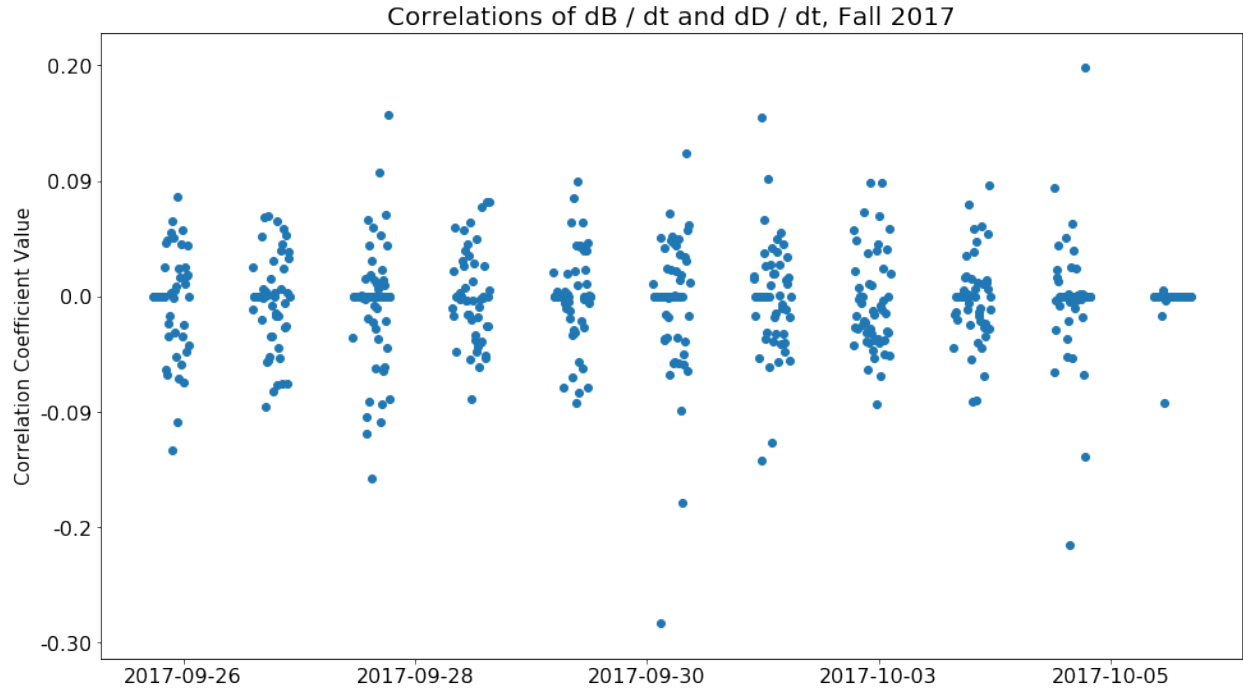


Figure 12: Correlation of change in bird density and change in brightness, between each timestep where there was a nonzero change in brightness and bird density, for 1.5 weeks in Fall 2017. Each night, the correlation coefficients appear to be randomly distributed about 0 with no temporal pattern, indicating no relationship between changing light and changing bird densities.

## 4 Conclusion

The relationship between building luminance and reflectivity is difficult to pinpoint given the spatial and temporal limitations of available radar data. However, this paper presents novel methodology in investigating the two variables' overlap both in aggregate and over time, detecting the presence of local scale trends and repeated temporal patterns. In order to process and analyze the data at scale, assumptions had to be made about uniform building brightness, the brightness of occluded buildings, and the isolation of bird signals from other non meteorological signals. In particular, looking at spatial correlations over time, there appears to be no relationship between either bird densities or changing bird densities

and light levels or changing light levels, respectively. Despite these limitations, there is some visual evidence of a relationship between luminance and reflectivity in short time scales that warrants further investigation. Further study would benefit from increasing the time range of the study, more heavily utilizing radial velocity in the differentiation of biological signals, closer investigation into locations of bird deaths, and a more thorough inference of building-level light emissions.

## 5 References

American Meteorological Society. Glossary of Meteorology. dBZ. <http://glossary.ametsoc.org/wiki/Dbz>

Crawford, Robert L. and Engstrom, R. Todd. (2001). Characteristics of Avian Mortality at a North Florida Television Tower: A 29-Year Study. *Journal of Field Ornithology*, 72(3):380-388. DOI: [http://dx.doi.org/10.1648/0273-8570\(2001\)072%5B0380:COAMAA%5D2.0.CO;2](http://dx.doi.org/10.1648/0273-8570(2001)072%5B0380:COAMAA%5D2.0.CO;2)

Dobler G, Ghandehari M, Koonin SE, Nazari R, Patrinos A, Sharma MS, et al. Dynamics of the urban lightscape. *Inf Syst* 2015;54:115–26.

Dokter AM, Felix L, Herbert S, Laurent D, Pierre T and Iwean H (2011). “Bird migration flight altitudes studied by a network of operational weather radars.” *Journal of the Royal Society Interface*, **8**, pp. 30-43.

Falchi F, Cinzano P, Duriscoe D, Kyba CC, Elvidge CD, Baugh K, et al. The new world atlas of artificial night sky brightness. *Science Advances*. 2016;2(6):1–25. doi: 10.1126/sciadv.1600377.

Gauthreaux, S.A. and C.G. Belser (1998). Displays of Bird Movements on the WSR-88D: Patterns and Quantification. *Wea. Forecasting*, **13**, 453–464, [https://doi.org/10.1175/1520-0434\(1998\)013&lt;0453:DOBMOT&gt;2.0.CO;2](https://doi.org/10.1175/1520-0434(1998)013&lt;0453:DOBMOT&gt;2.0.CO;2)

Gauthreaux, S.A., Livingston J. W., Belser, C.G (2008). Detection and discrimination of fauna in the aerosphere using Doppler weather surveillance radar. *Integrative and Comparative Biology*, Volume 48, Issue 1, Pages 12–23, <https://doi.org/10.1093/icb/icn021>

Herbert, A.D. 1970. Spatial disorientation in birds. *Wilson Bull.* 82:400–419.

Hubbert, J.C., M. Dixon, S.M. Ellis, and G. Meymaris (2009). Weather Radar Ground Clutter. Part I: Identification, Modeling, and Simulation. *J. Atmos. Oceanic Technol.*, **26**, 1165–1180, <https://doi.org/10.1175/2009JTECHA1159.1>

La Sorte, F. A., Hochachka, W. M., Farnsworth, Sheldon, D., Van Doren, B. M., Fink, D., Kelling, S. (2015). Seasonal changes

in the altitudinal distribution of nocturnally migrating birds during autumn migration. *R. Soc. open sci.* 2015 2 150347; DOI: 10.1098/rsos.150347.

La Sorte, F. A., Fink, D., Buler, J. J., Farnsworth, A., and Cabrera-Cruz, S. A. (2017). Seasonal associations with urban light pollution for nocturnally migrating bird populations. *Global change biology*, 23(11):4609–4619.

Miles W, Money S, Luxmoore R, Furness RW (2010) Effects of artificial lights and moonlight on petrels at St Kilda. *Bird Study* 57: 244–251.

Mouritsen, H., and O. N. Larsen. 2001. Migrating songbirds tested in computer-controlled Emlen funnels use stellar cues for a time-independent compass. *The Journal of Experimental Biology* 204:3855–3865.

Newton, Ian. 2008. *The Migration ecology of birds*. London, UK: Elsevier.

NOAA National Centers for Environmental Information. NEXRAD. <<https://www.ncdc.noaa.gov/data-access/radar-data/nexrad>> Accessed April, 2018.

NOAA Radar Operations Center (2017). NEXRAD Technical Information. <<https://www.roc.noaa.gov/WSR88D/Engineering/NEXRADTechInfo.aspx>> Accessed July, 2018.

NOAA National Weather Service. About our WSR-88D Radar. <[https://www.weather.gov/iwx/wsr\\_88d](https://www.weather.gov/iwx/wsr_88d)> Accessed July, 2018.

Poole, M., & O'Farrell, P. (1971). The Assumptions of the Linear Regression Model. *Transactions of the Institute of British Geographers*, (52), 145-158. doi:10.2307/621706

Stepanian, P. M., K. G. Horton, V. M. Melnikov, D. S. Zrnić, and S. A. Gauthreaux Jr. 2016. Dual- polarization radar products for biological applications. *Ecosphere* 7(11):e01539. 10.1002/ecs2.1539

Van Doren, Benjamin M., Horton, Kyle G., Dokter, Ariaan. M., Klinck, Holger., Elbin, Susan B., and Farnsworth, Andrew. (Oct 2017). High-intensity urban light installation dramatically alters nocturnal bird migration. *Proceedings of the National Academy of Sciences*. 114 (42) 11175-11180; DOI: 10.1073/pnas.1708574114

Verheijen, F. J. 1985. Photopollution: artificial light optic spatial control systems fail to cope with. Incidents, causations, remedies. *Experimental Biology* 44:1-18.

## 6 Data Sources

NOAA National Centers for Environmental Information (2017): Land Based Station Data. Accessed June 2018.

NOAA National Weather Service (NWS) Radar Operations Center (1991): NOAA Next Generation Radar (NEXRAD) Level 2 Base Data. KOKX. NOAA National Centers for Environmental Information. doi:10.7289/V5W9574V. Accessed April 2018.

NYC Audubon. Volunteer bird death count data. Access methods confidential. Accessed April 2018.

The City of New York: NYC 3-D Building Massing Model with Building Identification Number: ESRI Multipatch. Accessed April 2018.

The Urban Observatory at the NYU Center for Urban Science and Progress: imaging data from One Bryant Park/Bank of America Tower. Accessed April 2018.

## 7 7 Supplemental Materials

### 7.1 Further Literature Review

There remains a lack of consensus on what exactly draws birds to sources of artificial light at night, making contextual inference in the scope of this project somewhat challenging. It is unknown whether a bird experiences any primary attraction to light sources at night and therefore proceeds to fly to them or rather if the bird becomes spatially disoriented upon coincidentally reaching a sources of artificial light, resulting in aggregation (Herbert, 1970). To this end, it is not known whether *attraction* or *capture* is the more appropriate behavioral labeling, with birds losing either visual cues to the horizon or instead being functionally blinded by light

sources they enter (Verheijen, 1985).

Notably, the impact on artificial light at night on local bird populations, as opposed to migrant bird populations, is minimal. These “resident birds” are either significantly less affected or unaffected by artificial light in their environments, suggesting that adaptation to the presence of artificial light may be possible (Mouritsen et al., 2005). Regardless of the mechanism behind bird navigation and interference of artificial light, reduction in artificial light emission has been found to be beneficial to bird populations (Miles et al., 2010).

While a fair amount of research has been conducted both to describe and to analyze artificial light at night, many studies have historically maintained only a broad geospatial scale when considering ALAN. Recently, Falchi et al. describe the creation of a worldwide map of artificial sky luminance that considers global regions subjected to different categories of artificial light. The study notes the importance of low-angle, upward-pointing light sources as a primary cause of light pollution with a significant impact on night luminance (Falchi et al., 2016).

## 7.2 Visualization of Bird Density and Brightness

### *Background*

After analyzing the data from radar for bird density and from cameras for urban night brightness, we obtain the correlation between artificial light conditions and bird-related variables such as densities or deaths. In order to clearly and effectively communicate the

results of our research to interested audiences, a series of visualizations in both video and Carto Map are to be produced consisting of lower Manhattan maps and data points from each of our sources. Our final goal in this part of the project is an interactive map with time series data of bird densities and brightness for every lat/long point. Users can select a point on the map and view data information showing those changing variables with time at the bottom.

## *Data*

On one hand, brightness data for the observed buildings within the sight of the camera d6 on April 23, 2017, is used in making the time depended videos. On the other hand, the joining data of birds and lights in April 2017 is used in making the Carto map.

## *Methods*

To plot the brightness map for lower Manhattan, we need brightness not only for each building but for every point on the map. We use a method like interpolation to calculate brightness for all the points from buildings brightness

$$C_o = \sum \frac{C_i}{\sqrt{(X_i - X_o)^2 + (Y_i - Y_o)^2}},$$

in which  $C_o$  is the brightness for the point we calculated and  $C_i$  is the brightness for each building. In this case, we do not use an interpolation method because a building between  $C_o$  and  $C_i$  can shelter the light from  $C_i$  to  $C_o$ .



Figure 13: Visualization of the brightness of observed buildings (yellow area) within the sight of camera d6. The size of red circles shows the brightness of each building.

### 7.3 Radar Methods

In order to extract bird related observations from radar data, this study used bioRad, a package written to analyze and visualize biological signals in weather radar data (Dokter, 2011). The outputs of the bioRad package will be a PPI (Plan Position Indicator) plot, showing the specified variables over Manhattan, and tabular data, which translate the NEXRAD grid cells into a user specified point density of 100 meter distances, with each point containing information about the radar variables. The main variable of interest is reflectivity, a measure of the echo intensity, or power transmitted

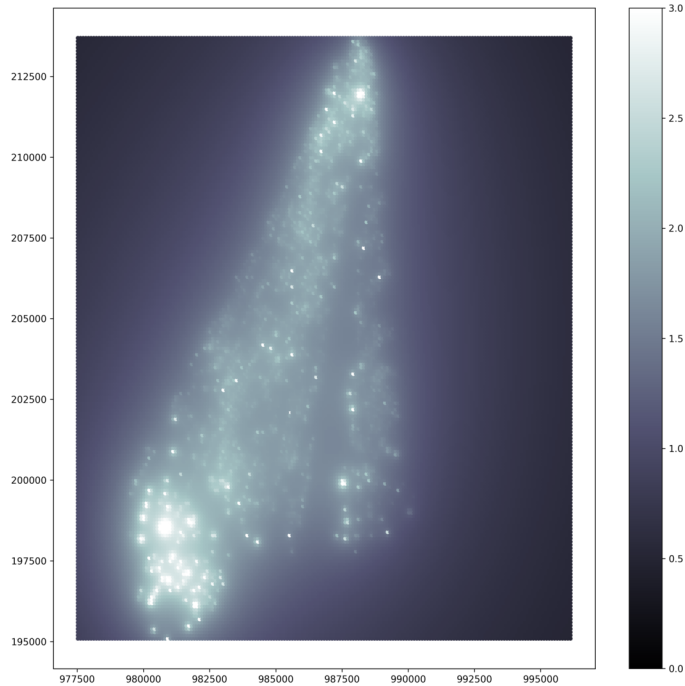


Figure 14: Visualization of brightness prediction in the area. In the video, users can observe how the brightness gets darker with time at night. It is obvious that the area of World Trade Center at the left bottom is the brightest portion.

back to the radar receiver. Reflectivity is a measure of density, and is measured on a logarithmic scale in DBZ, decibels relative to the reflectivity factor Z. A negative to under 20 range of DBZ means there is generally little density in the air, and around 20 would describe light rain (NOAA National Weather Service). The upper limit of reflectivity of birds is around 30 DBZ, so 35 DBZ will be chosen as a filter for the grid cells as a safe threshold (Stephanian, 2016).

Another variable of interest is the copolar correlation coefficient ( $\rho_{HV}$ ), which measures the correlation between vertically (DBZV)

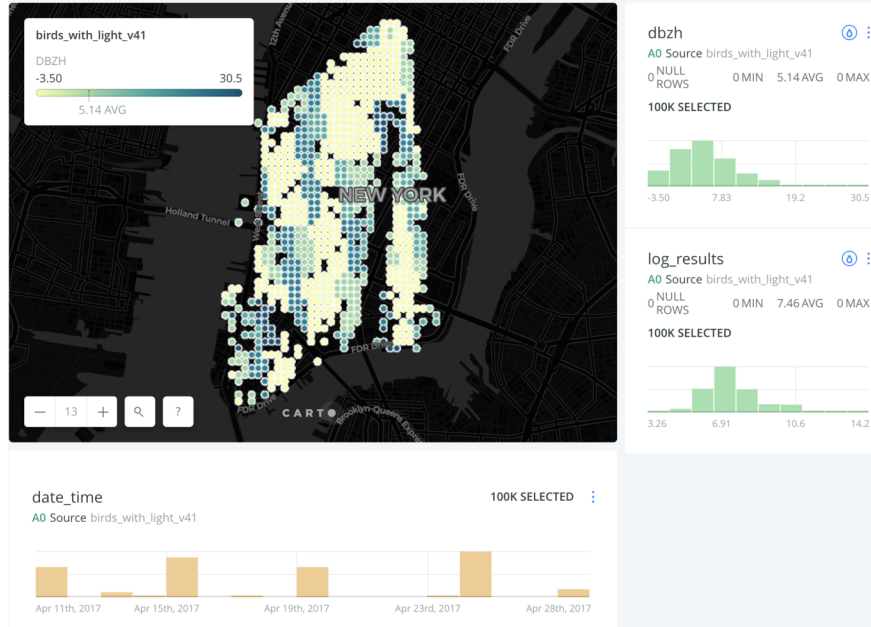


Figure 15: Carto map of bird density and brightness in April 2017. This is an interactive site in which users can either select a time period or select a variable to visualize. DBZH is the bird density reflectivity, and log\_results is the log of the sum of brightness within a 200 feet radius circle of the bird data point.

and horizontally (DBZH) polarized reflectivity factors. The correlation coefficient will be one if there is no pulse to pulse variation in a sampled volume, such as objects that are homogeneously dispersed, and will lower the more inhomogeneous the sample is. Because the shape and positioning of bird bodies is less homogenous than mist or rain drops, correlation coefficients of above 0.95 can be filtered out to remove meteorological observations from the study (Stephanian, 2016).

The last variable that will be examined is radial velocity, measured in meters per second. Velocity is useful for removing ground clutter, such as trees and buildings, that could be affecting results in reflectivity. As ground clutter is immobile, cells that have radial velocities within a range of -1 to 1 will be removed, although this could remove birds flying perpendicular to the radar as well (Hubbert, 2009). Ad-

ditionally, velocity has been used to distinguish birds from insects, as insects generally fly at speeds less than 8 to 10 meters per second, while migrating birds typically fly at speeds over 10 meters per second. However, due to the potential for overlap, this filter for insects will not be utilized (Gauthreaux, 1998).

## Bird Count Estimates

To estimate bird density, a similar methodology to Gauthreaux et. al. will be employed. Gauthreaux et. al. related maximum reflectivity values from 0.5° elevation scan angles to the number of birds crossing a 1.6 km line in an hour, which were observed by moon watching. This study resulted in a fit line that was a third order polynomial, and was found to be highly significant with an R-squared value of 0.87. Gauthreaux then went on to adjust the fit line, first converting migration traffic rates to density (birds per km<sup>3</sup>), and then converting relative decibels of reflectivity to just reflectivity (dBZ to Z). The result is a linear fit line, and when forced through zero, again generated an R-squared value of 0.87 (Gauthreaux et. al., 2008).

$$\frac{Birds}{km^3} = 1.84Z$$

This formula was adjusted for this project to accommodate different units and assumptions. As it was initially used to estimate bird counts in a square kilometer using maximum dBZ of the study area, the number of birds will be scaled down to the area of 100 meters, which is the spatial resolution of the radar data for this project. Additionally, dBZ (recorded by NEXRAD) will need to be converted to Z, which can be done using an anti-log (American Meteorological

Society). Using this equation, each radar observation, representing a 100m<sup>3</sup> area, will be able to have associated a number of birds within that area, creating an estimation of total birds. This estimate can then be summed over time to find the number birds in the study area

$$\frac{\text{Birds}}{100m^3} = \frac{\left(1.84 \cdot 10^{\frac{dBZ}{10}}\right)}{10}$$

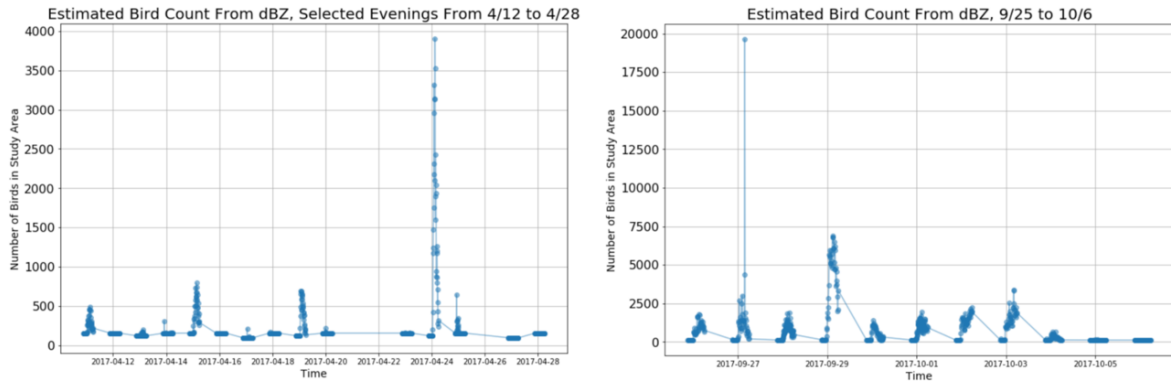


Figure 16: Estimated bird counts, relating reflectivity to bird densities summed within the study area.